https://doi.org/10.5194/tc-2020-206
Preprint. Discussion started: 17 August 2020

The Cryosphere Discussions

The cooling signature of basal crevasses in a hard-bedded region of the Greenland Ice Sheet

Ian E. McDowell[1], Neil F. Humphrey[1], Joel T. Harper[2], Toby W. Meierbachtol[2]

[1]Department of Geology and Geophysics, University of Wyoming, Laramie, Wyoming, 82071, USA
[2]Department of Geosciences, University of Montana, Missoula, Montana, 59812, USA

Correspondence to: Ian E. McDowell (ian.mcdowell@nevada.unr.edu)

Abstract. Temperature sensors installed in a grid of 9 full-depth boreholes drilled in the southwestern ablation zone of the Greenland Ice Sheet consistently record cooling over time within the lowest third of the ice column. Rates of temperature change outpace cooling expected from vertical conduction alone. Additionally, observed static temperature profiles deviate significantly from modeled purely diffusional thermal profiles, implying strong non-conductive heat transfer processes within the lowest portion of the ice column. Although numerous heat sources exist to add energy and warm ice as it moves from the central divide towards the margin such as strain heat from internal deformation, latent heat from refreezing meltwater, and the conduction of geothermal heat across the ice-bedrock interface, identifying heat sinks proves more difficult. After eliminating possible mechanisms that could cause cooling, we find that the observed cooling is a manifestation of previous warming in basal ice. Thermal decay after latent heat is released from freezing water in basal crevasses is the most likely mechanism resulting in the temporal evolution of temperature and the vertical thermal structure observed at our site. Basal crevasses are a viable englacial heat source in the basal ice of Greenland's ablation zone and may have a controlling influence on the temperature structure of the near basal ice.

1 Introduction

Rates of ice deformation and the onset of basal sliding are regulated by the thermal state of ice sheets (Hooke, 1981; Weertman, 1957), which makes ice temperature an important physical variable to be measured in the field and modeled to predict current and future ice motion. As ice moves from the central divide towards the margins, heat is conducted into the ice column from the surface and basal boundaries and is introduced through sources such as energy released by internal deformation and englacial refreezing of meltwater (Cuffey and Paterson, 2010).

Mechanisms of heat transfer and englacial heat sources in Greenland's ablation zone have been investigated by comparing sparsely collected temperature profiles to output from thermomechanical models (Iken et al., 1993; Funk et al., 1994; Luthi et al., 2002; Harrington et al., 2015; Luthi et al., 2015; Poinar et al., 2017). When attempting to replicate the vertical temperature structure, models consistently produce ice temperatures that are lower than collected temperatures (Luthi et al., 2002; Harrington et al., 2015; Luthi et al., 2015; Poinar et al., 2017). Previous modeling and observational studies highlight the appreciable influence of refreezing meltwater as a source of latent heat in Greenland's ablation zone (Phillips et al., 2013; Harrington et al., 2015; Luthi et al., 2015; Poinar et al., 2017; Seguinot et al., 2020). Outside of Greenland, observations of englacial warming from latent heat sources have been demonstrated as early as the 1970s (Jarvis and Clarke, 1974).

Here we investigate heat transfer processes using an extensive dataset collected from over 300 temperature sensors emplaced in a grid of 9 full-depth boreholes in southwestern Greenland. Rather than static snapshots of the vertical temperature field, our data provide sub-daily continuous records of ice temperature over a 2-3 year period. The high temporal and spatial resolution allow us to examine how the vertical thermal structure evolves in both time

https://doi.org/10.5194/tc-2020-206
Preprint. Discussion started: 17 August 2020

and space during the study period. Our continuous record of englacial temperatures allow us to identify dominant drivers of heat flow at our field location.

2 Methods

2.1 Field site

Nine boreholes were drilled in the southwestern portion of the Greenland Ice Sheet in a sector that discharges in the land-terminating outlet glacier, Issunguata Sermia. The field site is located approximately 33 km from the margin and has a surface elevation of 980 m above sea level with ice depth ranging from 640 m to 680 m. The dimensions of the borehole grid are approximately 250 m N-S and 500 m E-W. Figure 1 shows the layout of the instrumented field site.

Borehole experiments conducted immediately after drilling indicate the ice rests on bedrock with perhaps a veneer of sediment approximately a decimeter thick (Harper et al., 2017). Mean annual air temperature measured at the site is -10.5°C and ablation rates are 2-3 m yr^{-1} (Hills et al, 2018). Ice moves to the west (266°) at ~100 m yr^{-1} and inclinometry-derived deformation rates show that basal sliding comprises ~96% of ice motion, with internal deformation contributing the remaining 4% (Maier et al., 2019). Airborne radar measurements indicate that the bed elevation increases slightly from east to west across the site which indicates that the ice flows up a minor reverse bed slope (Paden et al., 2014).

2.2 Data collection

A hot water drill was used to melt boreholes ~10 cm in diameter through the full depth of the ice column. Cat-5 cables instrumented with digital temperature sensors were installed in the boreholes after drilling. These sensors were spaced every 10 m in the lowest 150 m of the ice column and every 20 m for the remainder of the depth. The uncalibrated accuracy of the sensors is 0.5 °C and the resolution is 0.0625 °C. We calibrated the sensors to improve the accuracy by reading the temperature of the water in the borehole immediately before refreezing, which is assumed to stabilize at the Clausius-Clayperon freezing point prior to complete freeze-up. With the freezing point field calibration, we are confident in the sensors' accuracy to approximately 0.1 °C. Data loggers at the ice surface recorded temperature readings every 4 hours between the date the borehole was drilled in either July 2014 or July 2015 and the end of the data collection period in July 2017. Each temperature measurement that the sensor records is an average of 64 temperature readings, which is then registered at the nearest resolution step of the sensor.

Our data allow us to examine both the static vertical temperature field within the ice column as well as the temporal changes in temperature. To display the ambient static vertical temperature field with minimal effects of the thermal disturbance from hot water drilling, we report temperatures collected one year after boreholes are drilled (Humphrey and Echlemeyer, 1990; Supplementary Materials).

The temporal records of temperature change we present also neglect the first year of measured temperatures to eliminate the drilling disturbance. After this time, the measurements of temperature in the electrically isolated environment result in a time series of temperature changes that is mostly noise-free and at the absolute limit of the sensor's resolution. The data is cleaned of the few readings recording more than $\pm$ 2 resolution steps from the

https://doi.org/10.5194/tc-2020-206
Preprint. Discussion started: 17 August 2020

preceding and succeeding measurements, since extreme jumps are likely caused by digital transmission errors between the sensor and data logger at the surface. Although englacial temperatures likely vary smoothly over time, the digital representation from sensor data shows temperatures changing over time in a stair-stepping pattern. Since the temporal temperature variations are small in relation to the sensor resolution, the data set is highly characterized by this stepped behavior. The rate of temperature change of a sensor is determined by a least squares regression of the data recorded over time. Linearly regressing our stepped data to determine the rate of change of temperature requires careful treatment to prevent a biased estimate from truncated observation periods (Supplementary Materials).

3 Results

The static vertical temperature field collected from the nine boreholes is shown in Fig. 2, with two boreholes only being instrumented with temperature sensors in only the lowest half of the ice column. Temperatures are lowest in approximately the middle of the ice column and increase towards both the surface and bed, with the lowest ~5 m reaching the pressure-melting point. To establish a depth reference for sensor comparison, and since we are most interested in near-basal ice temperatures, temperature profiles are plotted with respect to height above the bed.

Rates of temperature change are generally a function of position in the ice column (Fig. 3). A clear cooling signature is seen in the lowest third of the ice column in most boreholes, with some boreholes warming or cooling in locations outside of this region. Most boreholes cool at a rate of a few hundredths of a degree Celsius per year in the lowest portion of the ice column. Only five full-depth profiles are shown, as temperature sensors in boreholes 15N and 14W failed for most of the study period. Boreholes 15CB and 14SB were only instrumented in the lowest portion of the ice column.

While the observed temporal temperature changes are small, the trends are a real signal and not an artifact of sensor drift or random noise. Digital systems can exhibit both noise and drift over time; however, the expected magnitude of drift or aging is approximately an order of magnitude less than our observed trends. In addition, the coherence and lack of obvious bias in the data gives us confidence. We observe coherent packages of ice that cools (the bottom of 14SA, 14N, and 15CA) while other portions warm (top of 15CA and 14SA). Additionally, borehole pairs 14SA, 14SB and 15CA, 15CB are located within 10 m of each other and show similar rates and extent of cooling over time, establishing repeatability and viability of our measurements and methods.

4 Discussion

We focus on observed basal cooling, since cooling of ice near the bed is enigmatic. Multiple heat sources are available to warm ice as it flows from the interior towards the margins. Heat sinks, however, are not obvious, other than vertical thermal conduction from the relatively warm ice at the bed into the cold central core. We proceed by investigating the potential causes of cooling in the lower part of the ice column.

https://doi.org/10.5194/tc-2020-206
Preprint. Discussion started: 17 August 2020

4.1 Diffusive cooling driven by the observed static temperature field

We compare our observed static temperature profiles to a simple vertical thermal diffusion model to observe if the magnitude of observed cooling over time could be produced purely from vertical diffusion. We use the 1-D thermal diffusion equation in the vertical dimension:

$$\frac{\partial T}{\partial t} = k\frac{\partial^2 T}{\partial z^2} + \frac{(Q(z,t))}{\rho C} \quad (1)$$

Where T is temperature, and t is time; k, ρ, and C are respectively, the thermal diffusivity, density, and specific heat capacity of ice. We initially set the source or sink term, Q, to zero, so that only thermal diffusion occurs in our model. The spatial second derivative is derived from our observed temperature profile. The temperature data has small amounts of noise as well as calibration offsets between sensors. Derivatives of real data, with any noise or error, tends to amplify the noise. To reduce noise levels and focus on the large-scale characteristics, we smooth the profiles using a 5th degree polynomial. The full-depth observed rates of temperature change in Fig. 3 are also smoothed using a 5th degree polynomial to facilitate comparison between the changes in temperature expected from collected profiles.

Comparison of our data and the model indicates that the curvatures in our temperature profiles cannot produce the observed temporal changes of temperature over time through diffusive heat flow alone. To illustrate the discrepancies between modeled temperature changes caused by vertical thermal diffusion and the observed temporal temperature change, we calculate the additional sources or sinks of heat required throughout the ice column to sustain the observed temperature change through time. Figure 4 presents a vertical distribution of the required Q from the thermal diffusion calculations to produce the recorded temporal temperature changes. Although there is considerable variability, all boreholes require additional heat sinks within portions of the lowest half of the ice column, demonstrating that cooling near the bed cannot result from vertical thermal conduction alone.

We also apply similar thermal modeling to highlight the regions of the static profiles that are not only warming or cooling anomalously, but that may be warmer or cooler than could be expected for a thermal profile that had developed over time without heat sources or sinks within the profile. We use Eq. (1) to produce synthetic thermal states for each borehole at our site, assuming only diffusional processes occurred in the flow of ice from the ice divide to our site. The entire ice column is initially set to -20 °C, based on a collected temperature profile at the ice divide near Dye-3 (Gundestrup and Hansen, 1983). Boundary conditions are then applied, with the bed being set to the pressure-melting temperature, and the surface being set to the measured surface temperature of each sensor string. The model is run until the sum of absolute differences between the synthetic profile and collected profile is minimized for each borehole. This simple modeling fails to capture any of the effects of changing surface or basal boundary conditions in the ice flow from the divide. However, these synthetic profiles are useful to compare with the observed data, since the comparison tends to highlight thermal regions that reflect recent changes to either the boundary conditions or to non-modeled sources or sinks.

Discrepancies between collected and modeled temperature profiles for each full-depth profile used in the previous analysis are shown in Fig. 5. Noticeably, there are positive deviations in the lowest 100s of meters of the ice column, showing where the model cannot reproduce the relatively high temperatures in the lowest portion of our

https://doi.org/10.5194/tc-2020-206
Preprint. Discussion started: 17 August 2020

collected profiles. Observed cooling within the ice column is co-located with positive deviations from the model in three out of five full-depth boreholes (14SA, 14N, 15CA), revealing a strong signal of decreasing temperatures in ice that is warmer than model output in these three boreholes (Fig. 5). While the pattern of temporal temperature change in boreholes 15S and 15E is not as clear, sensors in 15S record cooling in warm ice near the bed, and ice in 15E slightly warms in some locations where ice is relatively cold.

4.2 Possible heat sinks

The pervasive cooling in ice warmer than our diffusion model output in some, but not all, of our borehole data is enigmatic, since multiple heat sources exist near the bed, but identifying heat sinks is problematic. In addition, the non-uniform nature of the cooling between boreholes requires explanation. We dismiss several possible heat sinks below.

4.2.1. Melting in basal temperate ice

Ice near the bed at our field site is at the calculated pressure-melting temperature. Some melting can occur in this temperate ice as the pressure field varies due to ice flow. Melting may contribute to cooling near the bed as heat is needed for the phase change. However, ice only reaches the pressure melting temperature in the lowest ~5-10 meters at our site, with an even smaller temperate layer upstream. This process cannot explain cooling outside of this small area near the bed.

4.2.2 Basal refreezing from a thinning ice column

The ice sheet thins slightly along flow at our field site; the bed elevation increases while the surface elevation remains relatively constant. With a lower ice overburden pressure, the pressure-melting temperature increases (Cuffey and Paterson, 2010). Any interstitial water present in the ice would then be colder than the new melting temperature. The water would refreeze and release latent heat into the surrounding ice, resulting in warming rather than cooling. Because the temperate layer is confined adjacent to the bed, this process would also be localized.

4.2.3 Downward advection of the cold central core

All full-depth temperature profiles display a characteristic cold central core (Fig. 2). Vertical compression caused by longitudinal and transverse extension or basal melting could shift the cold ice downwards, causing temperatures in the lowest 100 meters to decrease. Our sensors would fail to detect this cooling because they are mechanically coupled to the same package of ice through time after the borehole freezes. The sensors move with the ice and continue to record to temperature of the same section of ice through time.

Alternatively, vertically compressing ice would steepen thermal gradients and facilitate higher rates of heat flow into the cold core. With an average surface vertical strain rate of -0.0043 yr^{-1} at our site (Maier et al., 2019), the change in the temperature gradient would result in temperature changes orders of magnitude lower than observed.

https://doi.org/10.5194/tc-2020-206
Preprint. Discussion started: 17 August 2020

4.2.4 Long-term changes in boundary conditions

Our simple thermal modeling assumed constant boundary conditions, which is obviously incorrect. Variations in the boundary temperatures will propagate into the interior of the ice column. Here we address several of the most likely boundary temperature changes to assess how they could affect the temporal evolution of the ice at our site.

The Little Ice Age in Greenland occurred approximately 500 – 200 years ago, and surface temperatures were ~ 0.5 °C colder than present (Dahl-Jensen et al., 1998). Scaling the e-folding time and length-scale of 1-D thermal diffusion described in Eq. (1) is useful for examining the thermal influence of a heat source and is approximated based on the exponential behavior of the solution to the partial-differential equation. The length, δ, at which surface temperatures have significantly decayed is proportional to the square root of thermal diffusivity (k) and time (t):

$$\delta = \sqrt{kt} \tag{2}$$

The length-scale for changes in surface temperatures during the Little Ice Age 500 years ago is ~130 m, which suggests hardly any thermal signature from the surface boundary exists below ~ 400 m depth.

Equation (2) also provides an estimate of the timescale of diffusion, illustrating changes in ice temperature from the end of the last interglacial period would have diffused away through entire ice column after ~12,000 years.

The most significant thermal change to the basal boundary is the transition from frozen to temperate, which occurs upstream of our site. This change introduces a warmer basal boundary relatively recently in terms of the ice flow; however, this would create a region of colder ice near the bed that is being warmed by conduction from the warm bed, not cooled as we observe.

4.2.5 Changes in ice motion

The interior ice sheet, which is frozen to the bed, moves largely by internal deformation and accumulates heat near the bed where strain rates are highest. At our site ice moves primarily by basal sliding (Maier et al., 2019) and this strain heat source is removed. Downstream from the region where this transition from deformation to sliding occurs, the ice near the bed would lose the strain-derived thermal energy and would cool as the heat diffused upward into the cold core. Although the location of the upstream transition from a frozen to thawed bed conducive to basal sliding is not precisely known, it is on the order of 200 km up-glacier from our field site (MacGregor et al. 2016), which translates to several thousand years for ice flow. Any heat anomalies would have decayed using Eq. (2).

Although the frozen to sliding transition is probably the largest change to the strain heating term, analysis by Meierbachtol et al. (2016) shows a strong change in the basal shear stress regime approximately 75 km upstream of our site, where the basal shear stress decreases down-flow by a factor of 2. Again Eq. (2) can be used to argue the thermal impact is negligible at our site, especially since the bulk of the strain and therefore strain heating occurs close to the basal boundary, which forms a fixed boundary condition at a short length scale for heat flow. However, it does point out that variations in the basal boundary stress state can cause minor heating or cooling, which we cannot completely eliminate since basal conditions are not well known.

https://doi.org/10.5194/tc-2020-206
Preprint. Discussion started: 17 August 2020


The Cryosphere Discussions
Open Access
EGU

205 **4.3 Thermal decay from basal crevasses**

With the lack of obvious heat sinks, we investigate the possibility that the observed cooling in the lower depths of the ice occurs as thermal decay after latent heat is released from freezing water. Temporally and spatially uniform heating by refreezing of disseminated water would not lead to our observations, since horizontal thermal diffusion would not occur in laterally extensive sections of isothermal ice. However, widely spatially separated transient
210 heating events, such as dispersed basal crevasses or moulins, only warm local ice, leaving significant regions of colder, unheated ice to facilitate horizontal diffusion, allowing the heated ice to cool back to ambient temperature. Since heat would flow horizontally, not vertically, it would not be revealed by our vertical thermal diffusion modeling.

A similar pattern of cooling in ice warmer than the 1-D thermal diffusion model produces is found in the
215 upper portion of 14N (Fig. 4). Hills et al. (2017) discuss the thermal anomaly exhibited in borehole 14N; the authors recognized the relatively high temperatures of ice in the upper portion of the borehole when compared to others in the grid (Fig. 2) and noticed that temperature sensors recorded decreasing temperatures over time. Hills et al. (2017) attributed this localized thermal anomaly to a refrozen crevasse that was observed on the ice surface nearby. The lowest 100 m of ice in boreholes 14SA, 14N, and 15CA all exhibit nearly identical thermal characteristics to the
220 uppermost portion of 14N: ice is warmer than our model produces, and it cools through time.

Basal crevasses are planar features that can have a thermal influence on large regions of ice. Additionally, multiple crevasses could be formed in an area, similar to surface crevasses, and their propagation is likely vertically restricted above the bed, so they affect only the lower portion of the ice column. For these reasons, we focus on the thermal disturbance created by basal crevasses that allow the influx of a plane of water from the bed up into the cold
225 ice. The refreezing of this injected water releases heat into the surrounding ice. Accurately modeling the thermal disturbance created by a basal crevasse is hampered by our lack of knowledge of these features, since they have only been directly observed under mountain glaciers. Even one-dimensional thermal modeling in ice surrounding a crevasse requires knowledge of the width of the crevasse and the presence of other nearby crevasses, since closely spaced water filled crevasses greatly reduce the refreezing rate (Jarvis and Clarke,1974). In addition, even the
230 refreezing problem is complicated by the Stefan boundary condition as the thickness of the crevasse is reduced by refreezing.

We do not attempt detailed modeling of the thermal disturbance of basal crevasses at our field site, but we can approximate the thermal disturbance created by a single or by multiple basal crevasses to compare with our data. We are interested in the thermal behavior of ice in the region of a basal crevasse at times much longer than the
235 crevasse remained open, so we model the crevasse as an instantaneous planar heat source, considering only the total latent heat released during the refreezing. We examine the thermal disturbance at a long timescale in the half-space adjacent to the crevasse using an analytic solution presented by Carslaw and Jaeger (1959):

$$T(l,t) = \frac{Q}{2\rho C(\pi k t)^{\frac{1}{2}}} e^{\frac{-l^2}{4kt}} \quad (3)$$

https://doi.org/10.5194/tc-2020-206
Preprint. Discussion started: 17 August 2020

Here T is temperature, l is the linear distance away from the heat source, t is the time that has passed since the heat was released, Q is the amount of heat released per unit area of the plane, ρ, C, and k is the respectively the density, specific heat capacity, and thermal diffusivity of ice.

We assume a crevasse thickness of 1 m, matching the upper limit of previously observed basal crevasse widths (Harper et al., 2010). The release of heat initiates a wave of thermal energy propagating away from the source (Fig. 6A). The diffusion of the warming front causes ice temperature to increase before cooling asymptotically back to the ambient ice temperature (Fig. 6B). After the crevasse refreezes, the remaining period of warming is short compared to the timescale of cooling, thus the likelihood of temperature sensors installed in a previously crevassed area recording warming is low. To compare this theoretical result with our data, we average the rates of cooling observed in the lowest 100m of the boreholes and show the range of these averages in Fig. 6C. The theoretical curves depend strongly on the original size of the crevasse, and on the distance away from the crevasse; however, we have chosen values that show that this process can produce rates of cooling of the same magnitude observed in the borehole array.

It is tempting to define timescale for the basal crevassing using our extensive temperature data. However, such an attempt is under constrained since similar thermal signatures could be produced by many crevasse geometries and arrangements in time and space. Instead we examine the same crevassing scenario above as a baseline to investigate the amount of time elapsed since refreezing to produce observed cooling rates given various distances between boreholes and hypothetical crevasses. Equation (3) is solved for a range of time and linear distances from the heat source, and rates of temperature change over time are calculated. Equivalent rates of cooling could be produced from the decay of thermal energy released by a refrozen crevasse after approximately 20 – 30 years if the boreholes directly intersect the crevasse. The time elapsed is less if the boreholes do not intersect the refrozen crevasse. Although speculative, it is interesting that using a time scale of 10-30 years, assuming an ice velocity of 100 m yr^{-1}, the ice currently at our field site would have been 1-3 km up-glacier, which is a location of current surface crevasses and a significant change in slope.

Basal crevasses reaching 10s of meters above the bed can theoretically occur in glaciers with basal water pressures at or above ice overburden pressures (van der Veen, 1998). Longitudinal extension further facilitates crevassing over 100 m above the bed (van der Veen, 1998). Subglacial water pressures in Greenland's ablation zone have consistently been measured at or near ice overburden pressure (Iken et al., 1993; Meierbachtol et al., 2013; Andrews et al., 2014; Ryser et al., 2014), and have peaked at ~ 1.15 times the ice overburden pressure at our field location (Wright et al., 2016). Longitudinal extension, while not temporally or spatially prevalent, may result from ice flow over uneven bed topography or spatial changes in basal friction.

It is unlikely that a single basal crevasse is responsible for the cooling that we observe at the field site. More plausibly, the ice at our field site was fractured by multiple crevasses up-glacier. We cannot precisely determine the number or spacing of crevasses; however, a 1-D modeling analysis shows that three 1 m thick refrozen crevasses would lead to dispersed cooling over a large area of the bed after 20-30 years (Supplementary Materials). The 1-D temperature field evolution illustrates the abrupt warming that occurs during refreezing, followed by dispersed cooling surrounding the crevasses over time (Fig. 7). Thermal energy likely diffuses away

https://doi.org/10.5194/tc-2020-206
Preprint. Discussion started: 17 August 2020

from our field site in 3-dimensions, which would result in cooling that we have not captured in our vertical 1-D modeling. It is plausible that boreholes intersect these regions of ice that have been thermally altered by basal crevassing.

Moulins are unlikely to create the observed thermal observations. As a heat source, we conceptualize moulins as linear pipes that release thermal energy from the surface to the bed. Cooling in relatively warm ice is not observed throughout the entire ice column in each borehole, which we would expect to see from a linear heat source extending over the full ice depth. Moulins have been shown to migrate horizontally with depth (Holmund, 1988), which could possibly avoid this objection; however, numerous moulins would be needed to generate the cooling we observe in multiple boreholes. In the ablation zone surrounding Issunguata Sermia, moulins have a mean density of 0.1 per square kilometer (Smith et al., 2015), which suggests that it is unlikely that multiple moulins have thermally altered the instrumented block of ice with a surface area of ~ 0.125 km^2.

5 Implications

The existence of basal crevasses has not been widely considered outside of alpine settings; however, these features likely impact the bulk water storage, basal water flow, and ice rheology in Greenland's ablation zone. Harrington et al. (2015) examined full-depth ice temperature data collected in boreholes at a site down-glacier, but on the same flowline as this study, and found temperate layer growth could not be reproduced by thermal modeling incorporating strain heat and longitudinal compression. The authors suggest basal crevasses allow latent heat to be released well above the bed and create the thick temperate layer.

The creep parameter in flow laws is highly temperature dependent, thus basal crevasses could create regions of enhanced deformation. In addition, water content in basal temperate ice also influences rates of glacial ice deformation. A previous study at the down-glacier site, found a higher water content in the basal temperate ice layer revealed by ground-based radar, than is used in modeling studies (Brown et al., 2017). While unable to detect macro-spaces for bulk water storage in the radargrams, the authors speculated that basal crevasses provide macro-spaces for water storage based on the thermal evidence from Harrington et al. (2015), which results in the high water content observed.

Although basal crevasses have only been directly observed in the alpine setting, their existence under the Greenland Ice Sheet has strong implications for the basal hydrology. Basal crevasses have been observed creating englacial water flow above the bed (Harper et al., 2010) and even allowing complex three-dimensional crossing flow paths (Huzurbazar and Humphrey, 2008). These features have the potential to modulate subglacial discharge and efficiently transfer water through the subglacial drainage system.

6 Conclusion

Temperature measurements collected in 9 boreholes over 2-3 years show that ice cools in the lowest portion of the ice column, with all boreholes displaying cooling within the lowest third of the ice column. The main thermal sink is conduction of heat from this region up into the cold central core of the ice. Vertical diffusion modeling shows this cooling to be insufficient to explain our data. In addition, the thermal modeling shows the lowest section of ice in

https://doi.org/10.5194/tc-2020-206
Preprint. Discussion started: 17 August 2020

some boreholes is warmer than would be expected in a block of ice in Greenland's ablation zone. The observed cooling regions of the boreholes are located in the same regions of ice that are warmer than our diffusion model indicates.

After eliminating various potential heat sinks, we conclude the observed thermal anomalies are created by the cooling of basal ice that has been previously warmed by basal crevassing occurring upstream of our observation site. Latent heat released by refrozen basal crevasses locally warm ice near the bed, but the effects are distributed as thermal energy propagates outwards resulting in dispersed cooling at rates of the same magnitude as our observations. Our results provide additional thermal evidence for the existence of basal crevasses in Greenland's ablation zone, which has strong relevance for the temperature dependent rheology of the basal ice and intriguing implications for the complexity of the basal hydrologic system.

Data availability. Temperature measurements used in this manuscript are available at http://dx.doi.org/10.15786/20.500.11919/7147 (McDowell et al., 2020)

Author contributions. NH, JH, and TM designed the field study and installed temperature sensors. IM performed the analysis and wrote the manuscript with contributions from all co-authors.

Competing interests. The authors declare that they have no conflict of interest.

Acknowledgments. This work was funded by the National Science Foundation Office of Polar Programs-Arctic Natural Sciences awards #1203451 and #0909495. We thank Megan Thompson-Munson for her helpful discussions that improved the quality of the manuscript.

References

Andrews, L. C., Catania, G. A., Hoffman, M. J., Gulley, J. D., Lüthi, M. P., Ryser, C., Hawley, R. L. and Neumann, T. A.: Direct observations of evolving subglacial drainage beneath the Greenland Ice Sheet, Nature, 514(7520), 80–83, doi:10.1038/nature13796, 2014.

Brown, J., Harper, J. and Humphrey, N.: Liquid water content in ice estimated through a full-depth ground radar profile and borehole measurements in western Greenland, Cryosphere, 11(1), 669–679, doi:10.5194/tc-11-669-2017, 2017.

Carslaw, H. S. and Jaeger, J. C.: Conduction of Heat in Solids, 2nd ed., Clarendon Press., 1959.

Cuffey, K. M. and Paterson, W. S. B.: The Physics of Glaciers, Academic Press., 2010.

Dahl-Jensen, D., Mosegaard, K., Gundestrup, N., Clow, G. D., Johnsen, S. J., Hansen, A. W. and Balling, N.: Past Temperatures Directly from the Greenland Ice Sheet, Science, 282(5387), 268–271, doi:10.1126/science.282.5387.268, 1998.

Doyle, S. H., Hubbard, B., Christoffersen, P., Young, T. J., Hofstede, C., Bougamont, M., Box, J. E. and Hubbard, A.: Physical conditions of fast glacier flow: 1. measurements from boreholes drilled to the bed of Store Glacier, West Greenland, J. Geophys. Res.-Earth, 123(2), 324–348, doi:10.1002/2017JF004529, 2018.

Gundestrup, N. S. and Hansen, B. L.: Bore-hole survey at Dye 3, South Greenland, J. Glaciol., 30(106), 282–288, 1984.

Harper, J. T., Bradford, J. H., Humphrey, N. F. and Meierbachtol, T. W.: Vertical extension of the subglacial drainage system into basal crevasses, Nature, 467(7315), 579–82, doi:10.1038/nature09398, 2010.

https://doi.org/10.5194/tc-2020-206
Preprint. Discussion started: 17 August 2020

Harper, J. T., Humphrey, N. F., Meierbachtol, T. W., Graly, J. A. and Fischer, U. H.: Borehole measurements indicate hard bed conditions, Kangerlussuaq sector, western Greenland Ice Sheet, J. Geophys. Res.-Earth, 122(9), 1605–1618, doi:10.1002/2017JF004201, 2017.

Harrington, J. A., Humphrey, N. F. and Harper, J. T.: Temperature distribution and thermal anomalies along a flowline of the Greenland ice sheet, Ann. Glaciol., 56(70), 98–104, doi:10.3189/2015AoG70A945, 2015.

Hills, B. H., Harper, J. T., Humphrey, N. F. and Meierbachtol, T. W.: Measured horizontal temperature gradients constrain heat transfer mechanisms in Greenland ice, Geophys. Res. Lett., 44(19), 9778–9785, doi:10.1002/2017GL074917, 2017.

Hills, B. H., Harper, J. T., Meierbachtol, T. W., Johnson, J. V., Humphrey, N. F. and Wright, P. J.: Processes influencing heat transfer in the near-surface ice of Greenland's ablation zone, Cryosphere, 12(10), 3215–3227, doi:10.5194/tc-12-3215-2018, 2018.

Holmund, P.: Internal geometry and evolution of moulins, Storglaciaren, Sweden, J. Glaciol., 34(117), 1988.

Hooke, R. L.: Flow law for polycrystalline ice in glaciers: comparison of theoretical predictions, laboratory data, and field measurements, Rev. Geophys. Space. Ge., 19(4), 664–672, 1981.

Humphrey, N. and Echelmeyer, K.: Hot-water drilling and bore-hole closure in cold ice, J. Glaciol., 36(124), 287–298, 1990.

Huzurbazar, S. and Humphrey, N. F.: Functional clustering of time series: An insight into length scales in subglacial water flow, Water Resour. Res., 44(11), doi:10.1029/2007WR006612, 2008.

Iken, A., Echelmeyer, K., Harrison, W. and Funk, M.: Mechanisms of fast flow in Jakobshavns Isbrae, West Greenland: Part I. Measurements of temperature and water level in deep boreholes, J. Glaciol., 39(131), 15–25, 1993.

Jarvis, G. T. and Clarke, G. K. C.: Thermal effects of crevassing on Steele Glacier, Yukon Territory, Canada, J. Glaciol., 13(68), 243–254, 1974.

Lüthi, M., Funk, M., Iken, A., Gogineni, S. and Truffer, M.: Mechanisms of fast flow in Jakobshavn Isbrae, West Greenland: Part III. Measurements of ice deformation, temperature and cross-borehole conductivity in boreholes to the bedrock, J. Glaciol., 48(162), 369–385, 2002.

Lüthi, M. P., Ryser, C., Andrews, L. C., Catania, G. A., Funk, M., Hawley, R. L., Hoffman, M. J. and Neumann, T. A.: Heat sources within the Greenland Ice Sheet: dissipation, temperate paleo-firn and cryo-hydrologic warming, Cryosphere, 9(1), 245–253, doi:10.5194/tc-9-245-2015, 2015.

MacGregor, J. A., Fahnestock, M. A., Catania, G. A., Aschwanden, A., Clow, G. D., Colgan, W. T., Gogineni, S. P., Morlighem, M., Nowicki, S. M. J., Paden, J. D., Price, S. F. and Seroussi, H.: A synthesis of the basal thermal state of the Greenland Ice Sheet, J. Geophys. Res.-Earth, 121(7), 1328–1350, doi:10.1002/2015JF003803, 2016.

Maier, N., Humphrey, N., Harper, J. and Meierbachtol, T.: Sliding dominates slow-flowing margin regions, Greenland Ice Sheet, Sci. Adv., 5(7), eaaw5406, doi:10.1126/sciadv.aaw5406, 2019.

McDowell, I., Humphrey, N., Harper, J., and Meierbachtol T.: Full-depth ice temperature measurements from southwestern Greenland's ablation zone, 2015-2017, Mountain Scholar, doi: 10.15786/20.500.11919/7147, 2020.

Meierbachtol, T., Harper, J. and Humphrey, N.: Basal drainage system response to increasing surface melt on the Greenland Ice Sheet, Science, 341(6147), 777–779, doi:10.1126/science.1235905, 2013.

Meierbachtol, T., Harper, J. and Johnson, J.: Force balance along Isunnguata Sermia, West Greenland, Front. Earth Sci., 4(87), doi:10.3389/feart.2016.00087, 2016.

Paden, J., Li, J., Leuschen, C., Rodriguez-Morales, F. and Hale, R.: *IceBridge MCoRDS L1B Geolocated Radar Echo Strength Profiles, Version 2,* NASA National Snow and Ice Data Center Distributed Active Archive Center, doi: 10.5067/90S1XZRBAX5N, 2014.

https://doi.org/10.5194/tc-2020-206
Preprint. Discussion started: 17 August 2020

Poinar, K., Joughin, I., Lenaerts, J. T. M. and Van Den Broeke, M. R.: Englacial latent-heat transfer has limited influence on seaward ice flux in western Greenland, J. Glaciol., 63(237), 1–16, doi:10.1017/jog.2016.103, 2017.

Ryser, C., Lüthi, M. P., Andrews, L. C., Catania, G. A., Funk, M., Hawley, R., Hoffman, M. and Neumann, T. A.: Caterpillar-like ice motion in the ablation zone of the Greenland ice sheet, J. Geophys. Res.-Earth, 119(10), 2258–2271, doi:10.1002/2013JF003067, 2014.

Seguinot, J., Funk, M., Bauder, A., Wyder, T., Senn, C. and Sugiyama, S.: Englacial warming indicates deep crevassing in Bowdoin Glacier, Greenland, Front. Earth Sci., 8(65), doi:10.3389/feart.2020.00065, 2020.

Smith, L. C., Chu, V. W., Yang, K., Gleason, C. J., Pitcher, L. H., Rennermalm, A. K., Legleiter, C. J., Behar, A. E., Overstreet, B. T., Moustafa, S. E., Tedesco, M., Forster, R. R., LeWinter, A. L., Finnegan, D. C., Sheng, Y. and Balog, J.: Efficient meltwater drainage through supraglacial streams and rivers on the southwest Greenland ice sheet, P Natl Acad Sci USA, 112(4), 1001–1006, doi:10.1073/pnas.1413024112, 2015.

Thomsen, H. H., Olesen, O., Braithwaite, R. J., and Boggild, C.: Ice drilling and mass balance at Pakitsoq, Jakobshavn, central West Greenland, Report 152, Grønlands Geologiske Undersøgelse, Copenhagen, Denmark, 1991.

van der Veen, C. J.: Fracture mechanics approach to penetration of bottom crevasses on glaciers, Cold Reg. Sci. Technol., 27(3), 213–223, doi:10.1016/S0165-232X(98)00006-8, 1998.

Weertman, J.: On the sliding of glaciers, J. Glaciol., 3(21), 33–38, 1957.

Wright, P. J., Harper, J. T., Humphrey, N. F. and Meierbachtol, T. W.: Measured basal water pressure variability of the western Greenland Ice Sheet: Implications for hydraulic potential, J. Geophys. Res.-Earth, 121(6), 1134–1147, doi:10.1002/2016JF003819, 2016.

https://doi.org/10.5194/tc-2020-206
Preprint. Discussion started: 17 August 2020

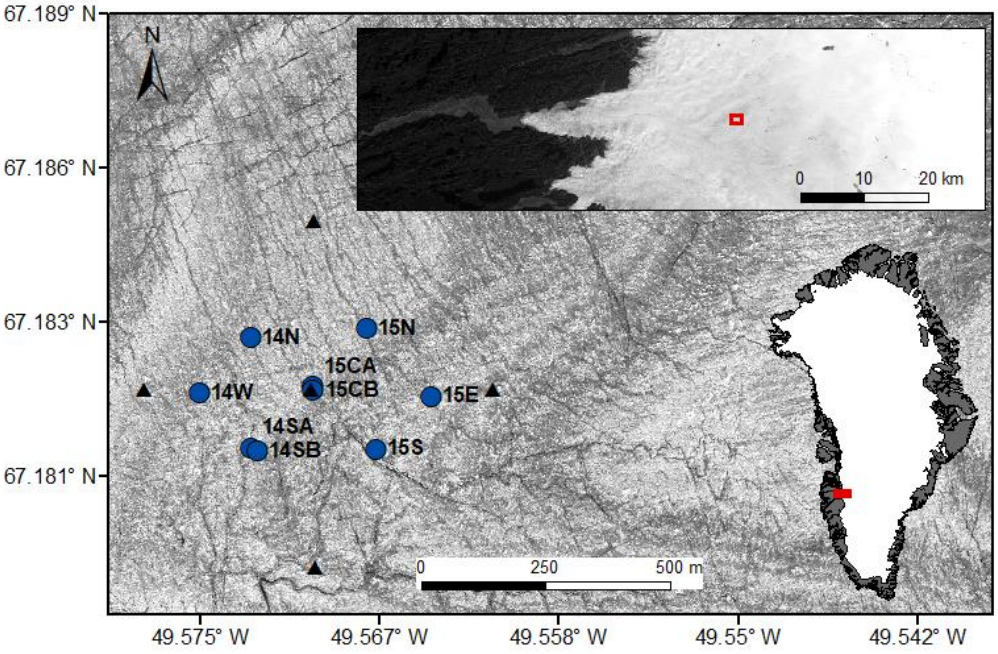

Figure 1: Map of the field location showing the layout of the 9 boreholes (blue dots) and the 5 GPS stations (black triangles). Borehole nomenclature is determined by the year that they were drilled and the direction from the center borehole and GPS station. The boreholes are located ~33 km from the margin of Issunguata Sermia outlet glacier (upper inset) in southwestern Greenland (lower inset). Boreholes are plotted on WoldView-2 image.

https://doi.org/10.5194/tc-2020-206
Preprint. Discussion started: 17 August 2020

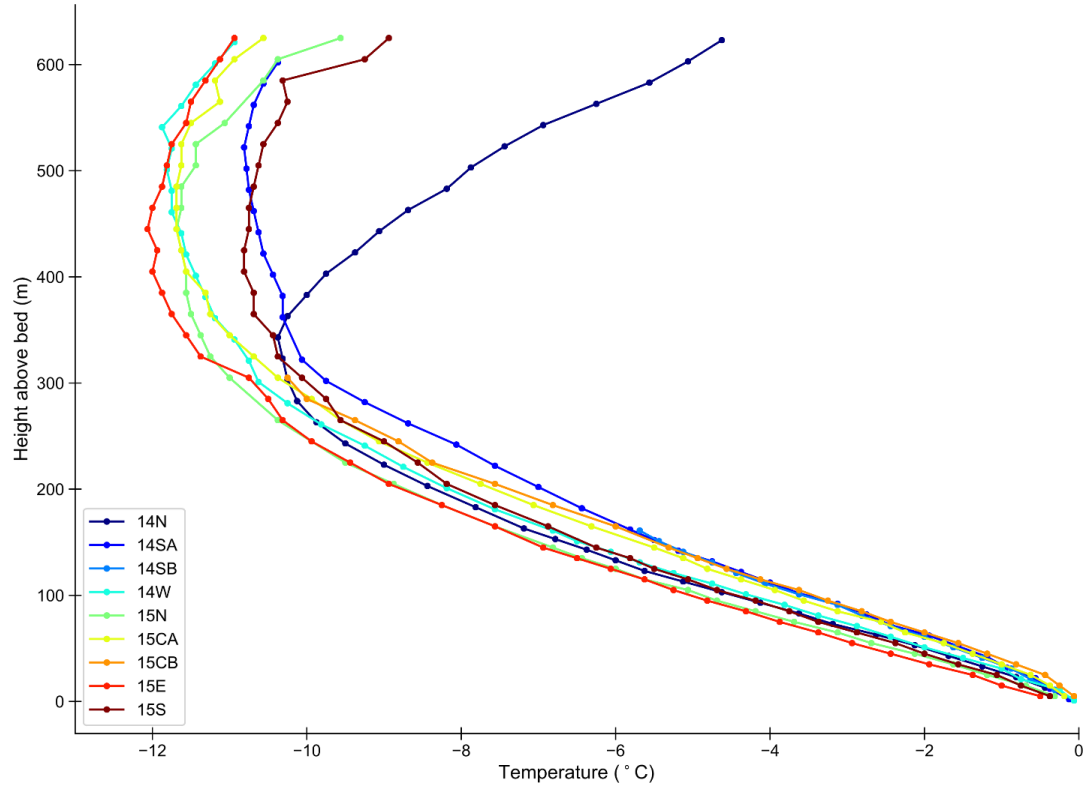

Figure 2: Temperature profiles for each borehole plotted with respect to each sensor's height above the bed. Sensor locations are marked with points and temperatures between sensors are linearly interpolated.

https://doi.org/10.5194/tc-2020-206
Preprint. Discussion started: 17 August 2020

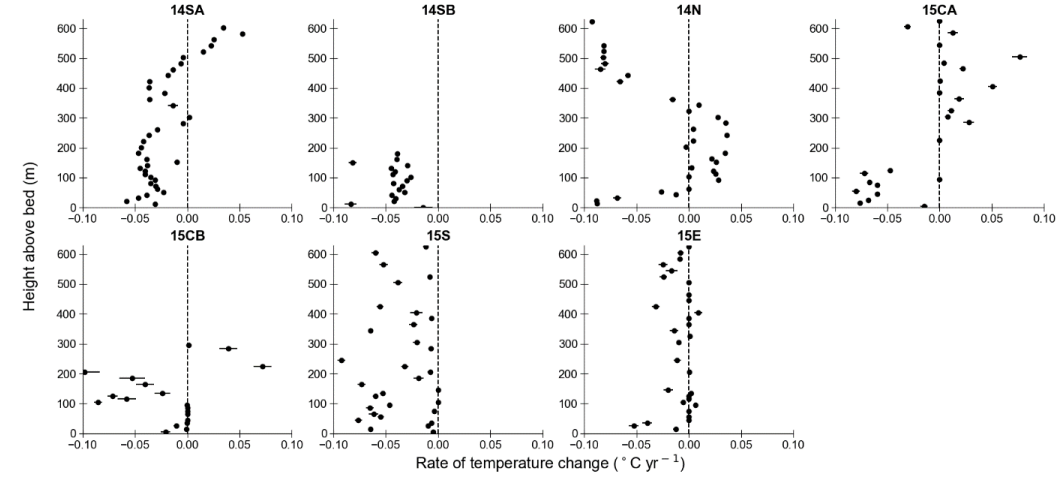

415

Figure 3: Rates of temperature changes for each borehole plotted against each sensor's height above the bed. Error bars indicate 2 standard errors from the mean rate, determined by the linear regression.

https://doi.org/10.5194/tc-2020-206
Preprint. Discussion started: 17 August 2020

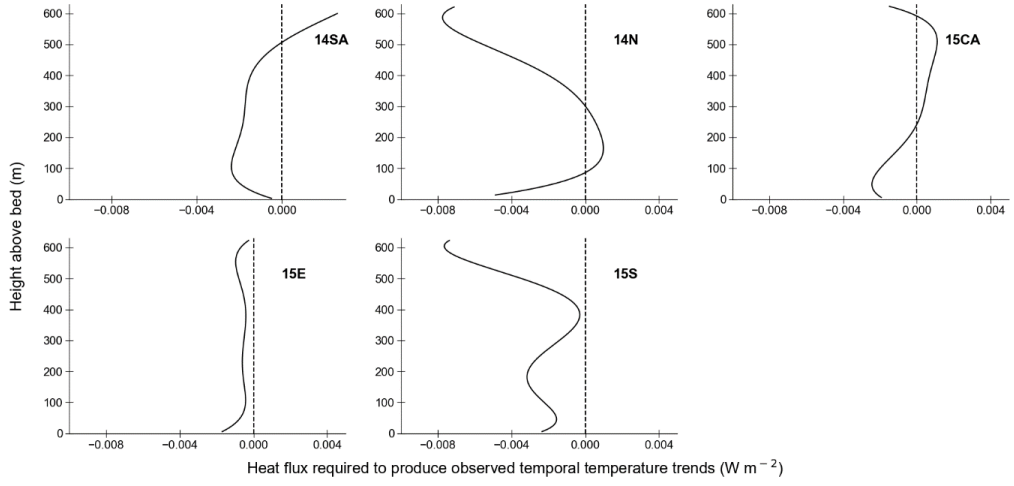

420

Figure 4: Additional heat fluxes required to maintain observed rates of temperature change if the collected static temperature profiles diffusionally evolve over time. Dashed line indicates the switch between a required heat source or sink.

https://doi.org/10.5194/tc-2020-206
Preprint. Discussion started: 17 August 2020

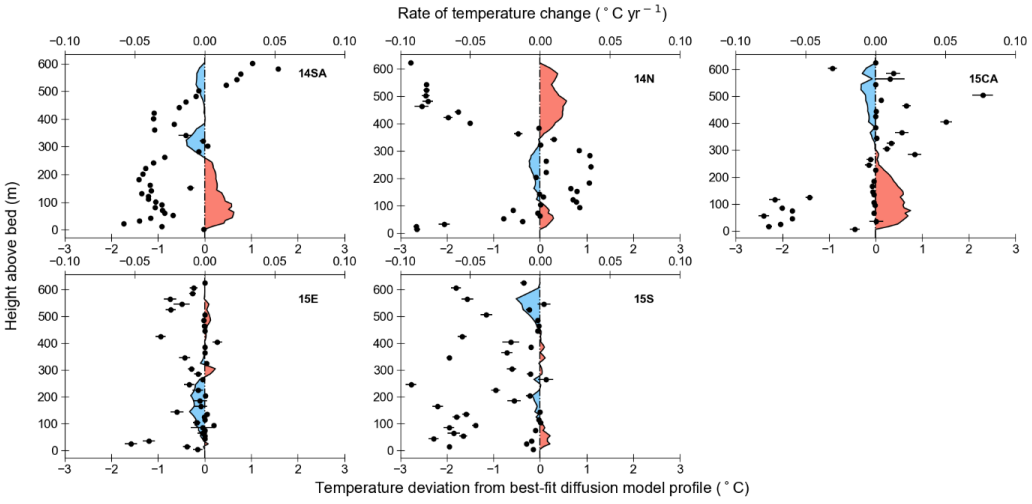

Figure 5: Rates of temperature change for each borehole (black dots) plotted with temperature deviations from the best-fit profile at each borehole. Red shaded regions indicate that the collected static profile is warmer than a pure diffusion profile, and blue shaded regions show the static profile is colder than the diffusion profile. Error bars on the calculated rates are the same as in Fig. 3. Only boreholes that have full-depth data are shown.

https://doi.org/10.5194/tc-2020-206
Preprint. Discussion started: 17 August 2020

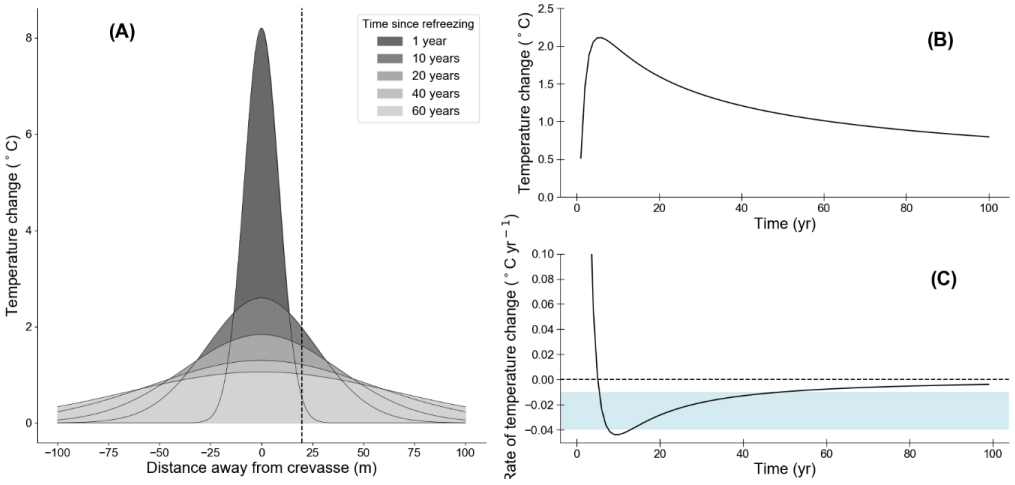

Figure 6: (A) Changes in temperature after a crevasse 1 m thick refreezes. Darker colors show earlier times. Dashed line indicates a distance 20 m from the crevasse, which temperatures and temporal rates of temperature change are shown in B and C. (B) Changes in temperature over time at 20 m away from the basal crevasse. (C) Corresponding rates of temperature change for panel B. The blue shaded region shows the range of averaged rates of cooling in the lowest 100 m of the boreholes.

425

https://doi.org/10.5194/tc-2020-206
Preprint. Discussion started: 17 August 2020

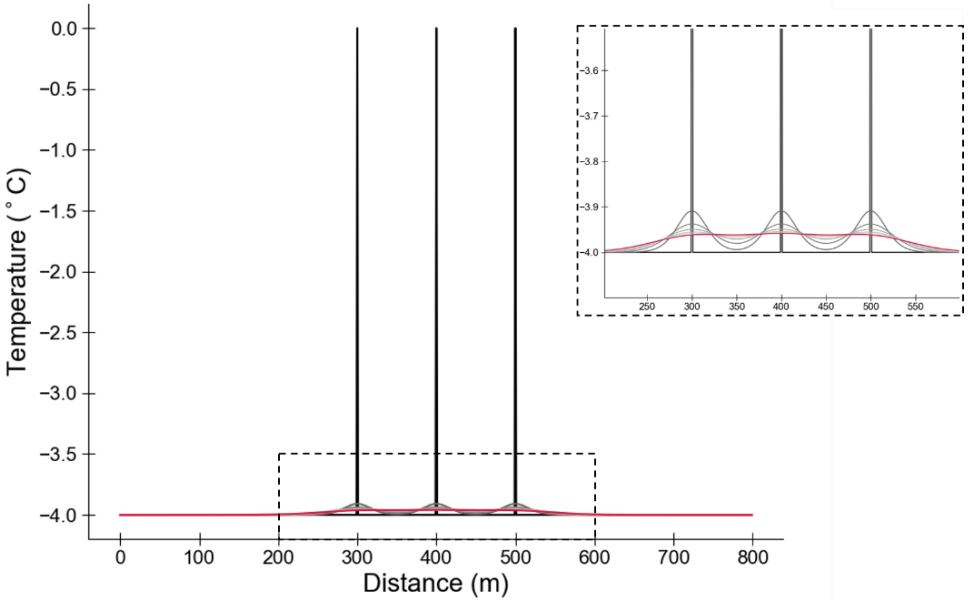

Figure 7: Evolution of a synthetic 1-D temperature field from basal crevasses spaced 100 m apart. Temperatures are plotted every 5 years, and older temperature fields are shaded darker shades of grey. Red line shows the temperature field 30 years after refreezing. Dashed box shows the extent of the inset figure, which shows large areas of the bed cool over time.